Spectrum of Engineering Sciences
ISSN (e) 3007-3138 (p) 3007-312X Volume 3, Issue 9, 2025

COMPUTATIONAL PREDICATIONS OF NON-NEWTONIAN FLUIDS THROUGH TWO-STEP RECTANGULAR BACKWARD DUCT

Ihsanullah, Mansoor Ali, Nisar Ahmed, Afshan Parveen Dehraj, Abdul Samad Shaikh, Dr. Hisam uddin Shaikh

M.Phil., Department of Mathematics, Shah Abdul Latif University Khairpur Mir's
seelroihsanullah@gmail.com
M.Phil., Department of Mathematics, Shah Abdul Latif University Khairpur Mir's
mansoorsangi422@gmail.com
M.Phil., Department of Mathematics, Shah Abdul Latif University Khairpur Mir's
nisarahmedsoomro385@gmail.com
Assistant Professor, GRA-GDC Kandiaro afshankb02@gmail.com
M.Phil. Scholar, Department of Mathematics, Shah Abdul Latif University Khairpur Mir's
samadshykh78@gmail.com
Professor, Department of Mathematics, Shah Abdul Latif University Khairpur Mir's

DOI: https://doi.org/

Keywords
Brand Communication on Social Networking Sites, Online Purchase Intention, Brand Attachment, Online Brand Experience

Article History
Received on 20 Aug 2025
Accepted on 27 Aug 2025
Published on 21 Sep 2025

Corresponding Author: *

Abstract
These days, mathematical modeling is common and crucial due to the medical sciences' urgent requirement to visualize the blood structure that travels through the human body's numerous vessels, veins, arteries, and other organs. Human diseases are on the rise, particularly stenosis, issues with the arteries, increased fat in the artery tubes, and high cholesterol that impairs blood flow through the veins and arteries. The channel's associated veins and arteries, as well as the ducts and tubes that joined them. Although blood is a very thick type of fluid, the non-Newtonian (NN) mechanics phenomenon was chosen in favor of the Navier-Stokes equations in two dimensions. As a result, the mathematical modeling of liquid movement via the double step backward channel was preferred. The momentum equation with pressure and velocity characteristics is favored, and these equations are condensed for liquid feature understandings. Owing to the intricate nature of the NN fluid problem, the computer tool COMSOL Multiphysics, which included the finite

element method, was selected for approximation modeling. In the sciences and engineering, this instrument plays a vital role in rapidly computing the steady state solution to challenging problems. The continuity equation with momentum equation was used to support the continuum method due to numerical modeling. Here, the flow characteristics are shown for the Reynolds number, which is a change in fluid resistance on velocity features, and the power law index rate, which is a change for viscosity calculations. It is concluded that eddies were seen at every stage and rapidly improved with a higher Reynold number and a lower index rate. On the other hand, eddies grow larger as the Reynolds number and index rate increase, but their size increases extremely slowly as they approach the double step channel's outlet.

Keywords: Non-Newtonian fluids; two-step backward duct; Reynolds number; power-law index; finite element method; computational fluid dynamics; COMSOL Multiphysics; flow separation.

INTRODUCTION

The single step backward channel flow phenomena is a very benchmark research problem and double backward step backward and forward step channel is a very new problem in the field of the fluid dynamics. Mostly literature found about the double step channel is the experimental analysis of water flow phenomena with mixing air flows. The double step backward channel found in the aircraft industries and relates to the ship like body of limited span available in the open-air environment. The problem is not limited but also relates in the marine industries with automotive engineering such as study of the complicated flow field phenomena near to the fight deck and in t design he auto motives vehicle industries to design the pickup truck that relates to the double step channels. Also, found in the hydraulic engineering for the construction in the filled (gabion) stepped weirs (Wang, et al. [2014] and Wuthrich and Chanson [2014]). The theme of the research problem to develop the approximate model of finite element analysis by the use of the Navier –

Stokes equations in two–dimension Cartesian coordinates (Amin, Said & Butt, 2025; Shah, Amin & Khan, 2025; Dash, et al., 2025). The finite element model is adopted here through the study of the CFD package COMSOL MultiPhysics and understand the flow phenomena of non-Newtonian fluids through the Power law model. The flow phenomena focused on the stream line laminar flow patterns, reattachment lengths and vortex observations in the corners of the double step backward channel.

Motivation

The problem focused on the PDE and these PDE are greatly applicable in the field of fluid dynamics in the shape of Navier–Stokes equations (NSE) such as momentum transport and continuity equations. Through NSE described the flow transport through the simple and complex domains. The flow may be liquid or gases or air. The domain of double backward step channel found in the various engineering and industries like hydraulic engineering, irrigation engineering and particular relates to the mining industries such as development the water flows through various canals and water ships such as object of finite span that is found in the open environment through air flows in which first step placed in between upper and lower deck and another second step found in between lower deck and surface of water.

Objectives Of the Study

To understand the phenomena of the mathematical modelling of governing equations and the predicted solution and will adopt the steady state solution through flow phenomena in the double step backward channel.

To require the comparison of the prediction of FE for the understanding the accuracy in the predicted solution with another predicted and experimental (if possible) of other researchers as given in literature.

To discuss further predictions of non-Newtonian fluid flow features to examine the behavior of fluids through the double step backward channel and proved the usages in the hydraulic engineering.

Literature Review

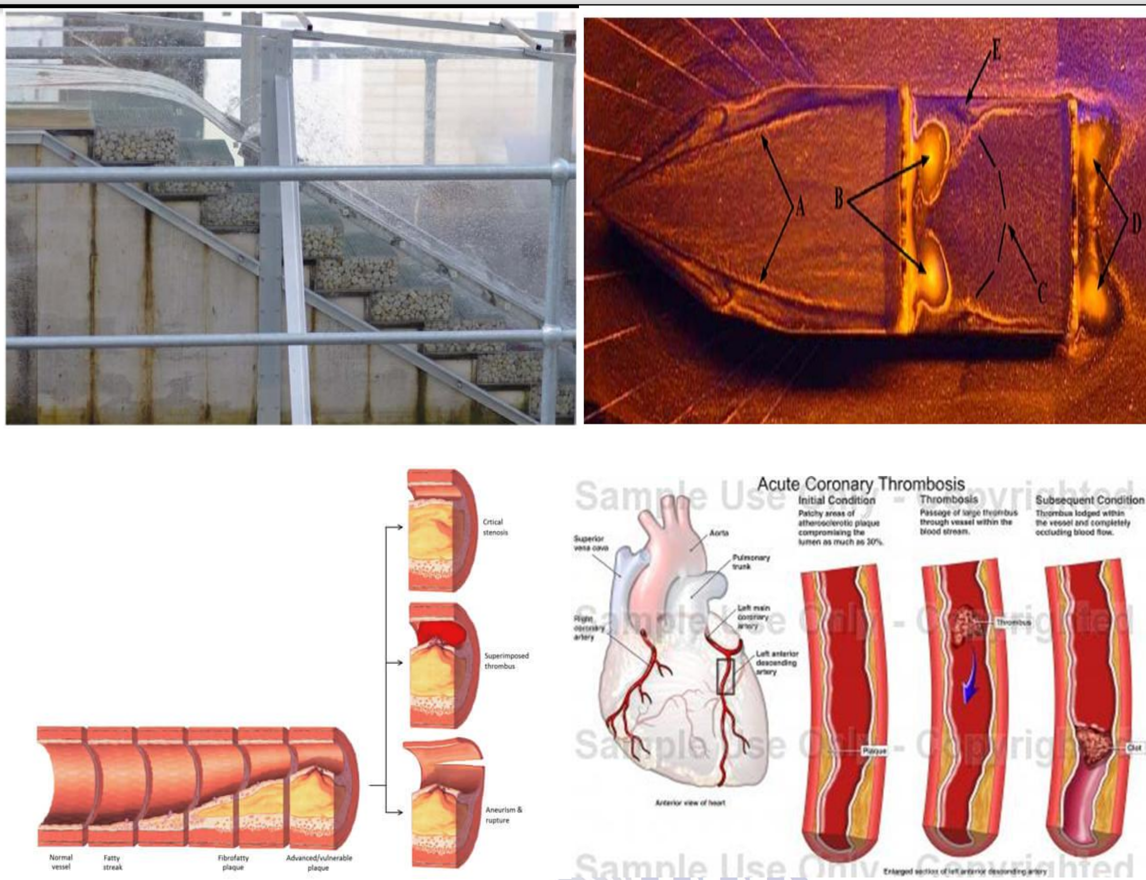

Figure – 2.1: Fluid flow through spillways and stenosis arteries.

These are the potential applications of water flows in dams and canals that relates to the research problem. Here the flow patterns are fully compared with the LSGFEM results. The behave is just like same appeared as eddies observed at each corner of the step flows (Elie,et al., 2014; Togun, et al., 2013; Wang, et al., 2014). Wruth and Chanson [2014], performed an air water flow experimental investigation through gabion stepped chute and also included impervious stepped chute with relatively ratio of 26.6^0 slope (1V:2H) and 0.10 m step height and the flow behavior was analyzed with Fraude similitude. It was concluded that for small discharges in the gabion stepped chute a porous region where the whole water has been seeped. Also, with the larger discharges in the case of gabion stepped chute three types of flow skimming, jet and transitional flows were founded. Moreover, it was also seen in the case of skimming flow the energy dissipation, the bubble count rate and turbulence intensity were also lower while the larger velocities were located at the downstream of gabion stepped weir. A theoretical and experimental investigation of the air turbulence flow through the backward step channel was conducted and compared with the inlet velocities obtained by the particle image velocimetry PIV with the use of Hot Wire Anemometry. Hall and Barber [2015] compared the both CFD and PIV results each other as both techniques were going to generate the statistics for turbulence, velocity and there might be a direct comparison of pressure contours and streamlines pattern of the velocity field. On comparing the components of velocities, vorticity and streamlines of CFD results of with PIV, it was recognized that CFD models are good fit to explain the flow regime in backward facing step channel. To observe the reattachment length Wang et al [2014] applied the Reynolds Average Navier Stokes model to analyze while the fluid is flowing through the two-dimensional double backward step facing channel by fixing the distance to height ratio (d/h) of the step from 0 to 10. The behavior of steady state flow was discussed by the vortex intensities, pressure as well as reattachment length. It was found through that two primary vortices are found at the corner of each step and a large vortex was found for the full large step of the channel. Togun et al. [2013], performed modeling and simulation with the help of finite volume-based software ANSYS Fluent 14 while dealing to observe the laminar and heat transfer flow in the double step backward facing step channel. Above and below wall of the channel was insulated and the three steps height is heated with constant Flux of 2000 w/m2 and the flow was analyzed 98.5 to 512 ranging Reynolds number. It was found that the Nusselt number shows the positive response with enhancing Reynolds number but shows negativity with the increase in step height. The results indicated that the heat transfer in the first step is more than the 2nd step due to increase in the vortex region in the 2nd step (Imtiaz, et al., 2025; Amin, et al., 2024; Imtiaz, Malik & Khan, 2024).

Steven [2016] keeping in mind that the analyzing the fluid flow behavior through the backward facing step channel is mostly under consideration because of being a benchmark problem, laminar flow regime or might be reporting and investigating the turbulence recirculation regions etc. Therefore, he suggested some parametric study which will give results comparable to experimental investigation. He suggested step height ranging from 10mm to 41mm, upstream height not more than 20h, expansion ratio 1.8h to 2h, total length of the channel might be 12h to 320h or the average value of the length 30h to 60h. Valero and Bung [2015], employed the new experimental and numerical study to observe self aeration process and aerated flow transport region while the air-water is passing through spillways which were fixed with the slopes 1:2. Different rates of flow or discharges were observed and also the most modern technologies like camera and ultrasonic sensors are used to see the air transport region and air water properties were reported respectively. For the numerical computation the RANS, RNG κ - ε turbulence modeling and volume of fluid VOF to observe the free surface trick have been applied. It was concluded that all the numerical parameters along with stagnation point, self-aeration process and energy dissipation were good when to compare experimental results except that of the velocities which were differed from the experimental calculation. Weiss et al. [2010], focused on influence of intrinsic three-dimensional properties of a separating as well as reattachment compressible flow when the fluid flow is allowing to pass through the three-dimensional circular cylinder with small diameter and then it shows the fluid flow behavior through the double backward step channel. Using a very high Reynolds number of 1.2 x10^6, the simulation has been performed to find the greatest coherent modes which creates the linear stability via two-point correlation. It was found that with the frequency f. D/u_{inf} =0.2 for a large-scale coherent motion exhibits a disordered separating and reattachment flow. Also, with the stability analysis it was deducted that axisymmetric turbulent impact after body dynamics is clearly influenced by instability with helical absolute and others for coherent modes 0 and greater 2 would have remained of convective nature. Results showed a good agreement with the pressure spectra governed through azimuthal antisymmetric geometries. The turbulent fluid flow and heat transfer of air through the 2D as well as 3D backward facing step channel with aspect ratio of 1.25 were examined by Smirnov et al. [2016] which used ANSYS Fluent CFD code and for a comparison purpose vortex resolving method IDDES at high Reynolds number of 28000. The RANS model of Mentor SST was used first with steady state computation to check the two and three-dimensional flow and then a time dependent study was done to check the impact of boundary layers due to the flow on sidewalls of the observed channel. The codes generated almost identical results with just a neglible difference of 4%. Furthermore, those results which were obtained through IDDES method were showing close agreement for wall fraction available through experimental data (Amin, 2025; Soma, et al., 2025; Amin, Daudpota & Khan, 2025).

To examine the quantitative as well as qualitative measurements for the fluid flow visualization through the 2D and 3D double backward facing step channel with particle image velocimetry and oil-flow visualization were used respectively by Tinney and Ukeily [2014]. A horseshoe vortex was seen along each step of the channel and also other vortical region were appeared in the geometry which create a large turbulence level can be seen at the center of the backward facing step channel whose mean square level greater than 2D flow. Also, it was deducted that due to the quasi-periodic shedding caused by the turbulence fluctuation draws energy continuously from the spirals produced at the nodes. Knowing to the industrial usage and MEMS application of the backward facing step channel, a fluid flow analysis was done for 2D and 3D by Haque et al. [2007] with the finite volume method with the implementation of segregated approach with simple scheme caused by velocity and pressure coupling. The flow was considered as turbulent and governing equations of all turbulent models were tested to predict the reattachment length produced at the corner of backward facing step channel. It was concluded that the ε based models produced the reattachment length was unpredictable when to compare with experimental observations for 2D and 3D flows. However, SST models present reattachment length to some good accuracy when to compare with the available literature. It was also seen that in 3D separation point was constant but reattachment points varied due to turbulent nature in 3D.

Study of the Governing Equations of Fluids Transport and the Finite Element Procedure

The governing equations relates to the convection – diffusion models with various type of boundary conditions are very strong and complicated research problem. Therefore, it is not easy to compute the exact solution in required time duration. Furthermore, unbalanced necessary initial and boundary conditions caused by the failure solution in analytical approaches. Through the invention of the computational languages, coding and various tools in the applied sciences, the complicated procedure of convection – diffusion models became easy to solve with regular and irregular boundary conditions with approximate techniques (Amin, 2025). These techniques provided the discrete values of the different unknowns through the mesh structures of the rectangular systems. Vast type of approximate technique methods are originated in the sciences and engineering problems and have different procedure adopted in the numerical methods, it may be finite difference methods that employed point to point wise distances approaches in a mesh structures and other one is finite element method that is appropriate numerical method for structured and unstructured meshes solution of convection diffusion models practically (Kwon and Bang [2000] and Jan, et al. [2016]). The merits of FEM is to easily handled through the computer algorithms and investigated converge solution with easy analysis of the convection – diffusion models.

This tool is vastly available in the study of the CFD field surveys with the controlling through computational programming such as C or C++, many computational codes of FEM available through FORTRAN and Matlab. Also, many strong computational packages available such as COMSOL Multiphysics. FEM provided the good and easy quick discretize the convection diffusion problems via many computational tools as stated under;

Concept of Mathematical Model for Fluid Dynamics

The concept of mathematical model is discussed in this chapter that models focused on the higher order partial differential equation and these PDE's are very strongly incorporated in the vast areas of the fluid and mass transport in the closed geometries such as channels and ducts. These equations are shortened as continuity equations that assumed the flow remained continuous in the closed geometries and other one momentum Brinkman equation that greatly available in the fluid movement with couple of various fluid parameters. Here discussed the two–dimension problem and constant density type fluids with varying viscosity of the fluids as described mathematically,

Equation of Continuity

This equation is used for the solenoidal vector fields that relates on the first order partial differential equation in which involve the velocity field in two – dimension and here just initiated for examine the continuous liquid fluids into the double step backward channel.;

$$\frac{\partial \lambda_1}{\partial x} + \frac{\partial \lambda_2}{\partial y} = 0 \tag{3–1}$$

Though, χ is prescribed for the velocity field that are solenoidal vector.

Model for the Momentum Transport

This model equation is most well known in the fluid dynamics phenomena that known as conservation law of momentum and also it is derived from well aware newton's law of motions (2^{nd} law). The fluid properties based mathematical model is defined as follows;

$$\rho\frac{D\lambda_1}{Dt} = \rho g_x - \frac{\partial P}{\partial x_i} + \frac{\partial}{\partial x}\left[\mu\left(\frac{\partial \lambda_1}{\partial x}\right)\right] + \frac{\partial}{\partial y}\left[\mu\left(\frac{\partial \lambda_2}{\partial y}\right)\right] + \frac{\partial}{\partial z}\left[\mu\left(\frac{\partial \lambda_3}{\partial z}\right)\right] \tag{3 – 2a}$$

$$\rho\frac{D\lambda_2}{Dt} = \rho g_y - \frac{\partial P}{\partial y} + \frac{\partial}{\partial x}\left[\mu\left(\frac{\partial \lambda_1}{\partial x}\right)\right] + \frac{\partial}{\partial y}\left[\mu\left(\frac{\partial \lambda_2}{\partial y}\right)\right] + \frac{\partial}{\partial z}\left[\mu\left(\frac{\partial \lambda_3}{\partial z}\right)\right] \tag{3 – 2a}$$

$$\rho\frac{D\lambda_3}{Dt} = \rho g_z - \frac{\partial P}{\partial z} + \frac{\partial}{\partial x}\left[\mu\left(\frac{\partial \lambda_1}{\partial x}\right)\right] + \frac{\partial}{\partial y}\left[\mu\left(\frac{\partial \lambda_2}{\partial y}\right)\right] + \frac{\partial}{\partial z}\left[\mu\left(\frac{\partial \lambda_3}{\partial z}\right)\right] \tag{3 – 2c}$$

The above system is called the general form of all type of liquid flows that the velocity filed is directly proportional to the pressure and for all types of flow like steady state and transient solutions. Also involved the various fluid properties such as density and viscosity. This model involved the couple of unknowns and fluid properties so not possible to compute the analytical or computational solution in this system. For the predicted solution, it is necessary in the fluid dynamics, to convert the dimension into non – dimensions form of the above system and introduce the non – dimension number as Reynolds number. Due to this invention, all fluid properties are removed from the above system (3 – 2), the new system becomes as;

$$\frac{\partial \lambda_i}{\partial t} + \lambda_j \frac{\partial \lambda_i}{\partial x_j} = -\frac{\partial P}{\partial x_i} + F_x + \frac{1}{\text{Re}}\left(\frac{\partial^2 \lambda_i}{\partial x_j\, \partial x_j}\right) \qquad i = 1, 2 \qquad j = 1, 2 \qquad (3\text{–}3a)$$

$$\frac{\partial \lambda_i}{\partial t} + \lambda_j \frac{\partial \lambda_i}{\partial x_j} = -\frac{\partial P}{\partial y_i} + F_y + \frac{1}{\text{Re}}\left(\frac{\partial^2 \lambda_i}{\partial x_j\, \partial x_j}\right) \qquad i = 1, 2 \qquad j = 1, 2 \qquad (3\text{–}3b)$$

Although, only introduce the dimensionless number that is known as;

$$\text{Re} = \frac{\rho \times u_{avg} \times L}{\mu}$$

Above fluid properties notations are described in the list of abbreviation and symbols in this thesis.

Initial and boundary Conditions

As the solution focused on the numerical computations in the required area of the geometry as double so that highly necessary to define the appropriate boundary conditions for the whole geometry as double step backward channel with focused on the initial condition for the iterative solutions. The following table shows the detail boundary conditions;

No. of zones	Initial condition	Boundary conditions
Stationary walls		No – slip boundary conditions as u = v = 0
Outlet		u = v = ?, P = 0
Inlet	$u(y) = 6 \times U_m \times \frac{y}{L}\left(1 - \frac{y}{L}\right)$ $P = P_{max}$	

Computational procedure Adopted VIA COMSOL Multiphysics

MILIEU

The computational procedure is taken through the numerical technique as finite element method and defaulted through the very strong and latest package COMSOL MultiPhysics. The complete process is as under;

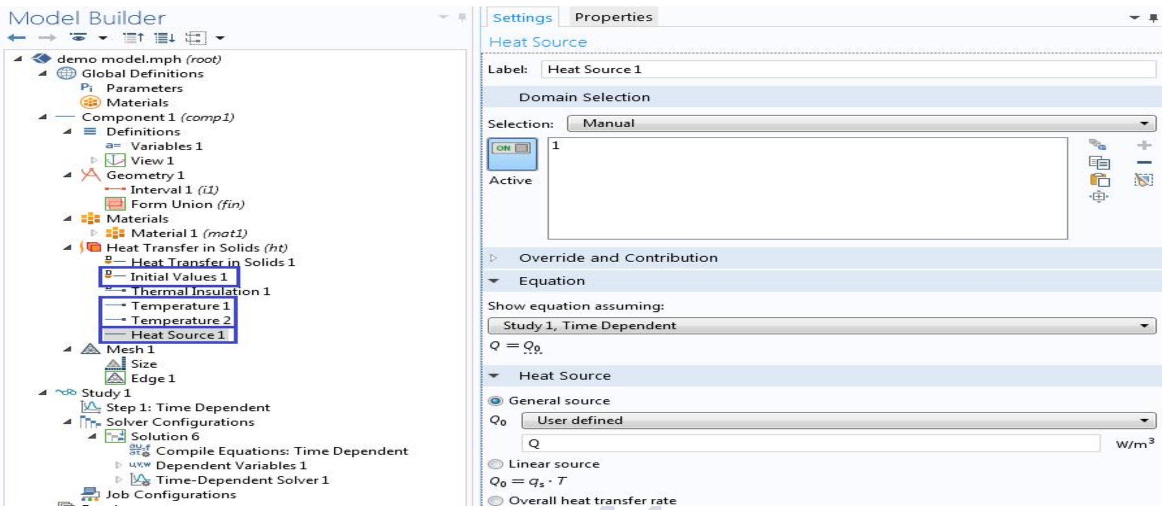

Figure – 3.1: menu bar of the problem defining in the COMSOL Multiphysics

In this menu bar, the procedure is completely defined from parameters to visualise the velocity and pressure flow patterns of every component. Initially, designed and defined the parameters list in the parameter menu bar such as fixed the fluid type, flow behave type, length and width of the geometry, appropriate initial and boundary conditions and etc. as per requirement. After that, defining the variables, set the geometry with the choice of the finite elements either course, fine and extremely fine mesh for the most accurate numerical solution and then compute the solution with the choice of the Newton's method.

Finite Element Method

Mostly, time – dependent problems involved the space with satisfied the physical laws are relates to the mathematical theory of the partial differential equations in 2nd order phenomena. Many more irregular type geometries and non – linear type problems found almost impossible to finalise the exact solution. Alternatively, the choice is the predictions through the various type of discretization procedure. Finite element method is the best choice for the real-life fluid motion equation solution approximately. Main theme of the FEM is to change the partial differential equations towards the variety of the linear discrete variable equations that can be easily handled through vast procedure of matrices through the computer systems. Basically, anybody closed either any dimension is theoretically piece wise up to limited number towards the small piece of the closed body known as elements or finite elements. The elements are supposed to be interconnected to each one called as nodes and series of regular or irregular nodes in a rectangular form is called the grid or mesh.

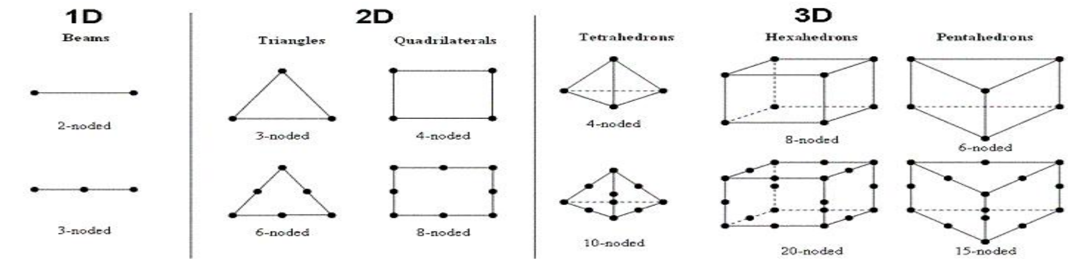

Figure – 3.2: type of the finite element method in different dimensions

The procedure shows a component described into the series of collection of finite elements called as discretization.

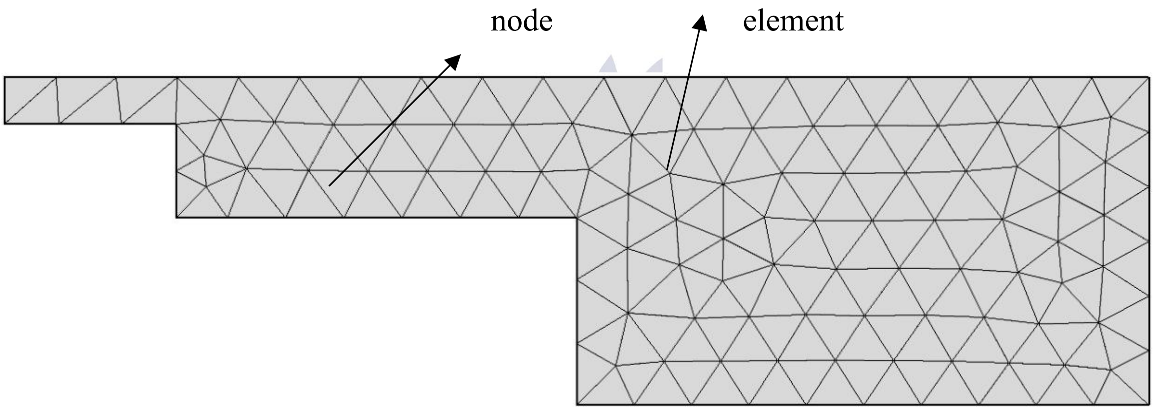

Figure – 3.3: grid style of the combined various rectangles.

COMSOL Process Adopted for the Governing Equations

The process adopted here through the Computational implement COMSOL Multiphysics and this procedure is taken through the finite element analysis coupled with the least square technique. This complete technique is just implemented on the linear order differential equations. But here the problem is higher order so assumed the extra components in the differential equations to transform higher order towards the linear order system of equations. The original problem of this project is clarified as below;

$$\nabla . \lambda = 0 \qquad (3-4)$$

$$-\frac{1}{\mathrm{Re}}\nabla^2 \boldsymbol{\lambda} + \nabla P + \boldsymbol{\lambda}(\nabla \boldsymbol{\lambda}) = 0 \qquad (3-5)$$

The new component extends in the velocity fields as vorticity that is known as;

$$\boldsymbol{w} = \nabla \times \boldsymbol{\lambda} \qquad (3-6)$$

Substitute the extra component vorticity $(3-6)$ into the other higher order differential equations $(3-4)$ and $(3-5)$

$$\nabla . \boldsymbol{\lambda} = 0 \qquad (3-7a)$$

$$\boldsymbol{\lambda} . \nabla \boldsymbol{\lambda} + \frac{1}{\mathrm{Re}} \nabla \times \boldsymbol{w} + \nabla p = 0 \qquad (3-7b)$$

$$w - \nabla \times \boldsymbol{\lambda} = 0 \qquad (3-7c)$$

The above system $(3-7)$ is employed for the general purpose of the fluids but the research project is limited, only two – dimensional in Cartesian form and also comprised on the constant density and change in viscosity of the fluids.

$$\frac{\partial \lambda_1}{\partial x} + \frac{\partial \lambda_2}{\partial y} = 0 \qquad (3-8a)$$

$$\lambda_1 \frac{\partial \lambda_1}{\partial x} + \lambda_2 \frac{\partial \lambda_1}{\partial y} + \frac{\partial P}{\partial x} + \frac{1}{\mathrm{Re}} \frac{\partial w}{\partial y} = 0 \qquad (3-8b)$$

$$\lambda_1 \frac{\partial \lambda_2}{\partial x} + \lambda_2 \frac{\partial \lambda_2}{\partial y} + \frac{\partial P}{\partial y} - \frac{1}{\mathrm{Re}} \frac{\partial \lambda_2}{\partial x} = 0 \qquad (3-8c)$$

$$w + \frac{\partial \lambda_1}{\partial y} - \frac{\partial \lambda_2}{\partial x} = 0 \qquad (3-8d)$$

The system $(3-8)$ is needed to transform into the least square approaches so it should be required to convert the above system into the matrix system through coefficients as below;

$$A_1 = \begin{pmatrix} 1 & 0 & 0 & 0 \\ \lambda_1 & 0 & 1 & 0 \\ 0 & \lambda_1 & 0 & -\frac{1}{\mathrm{Re}} \\ 0 & -1 & 0 & 0 \end{pmatrix}, \qquad A_2 = \begin{pmatrix} 0 & 1 & 0 & 0 \\ \lambda_2 & 0 & 0 & \frac{1}{\mathrm{Re}} \\ 0 & \lambda_2 & 1 & 0 \\ 1 & 0 & 0 & 0 \end{pmatrix}$$

$$A = \begin{pmatrix} 0 & 0 & 0 & 0 \\ 0 & 0 & 0 & 0 \\ 0 & 0 & 0 & 0 \\ 0 & 0 & 0 & 1 \end{pmatrix}, \qquad f = \begin{pmatrix} 0 \\ 0 \\ 0 \\ 0 \end{pmatrix}, \qquad \boldsymbol{\lambda} = \begin{pmatrix} \lambda_1 \\ \lambda_2 \\ p \\ w \end{pmatrix}$$

As the procedure for the least square residuals are defined as below to compute the stiffness matrix through KU = f

$$L\Psi_j = \Psi_{j,x} A_1 + \Psi_{j,y} A_2 + \psi_j \Psi \qquad (3-9a)$$

$$K_e = \int_{\Pi_d} \langle L\Psi_1, L\Psi_2, L\Psi_3, \ldots, L\Psi_{Ne} \rangle^T \langle L\Psi_1, L\Psi_2, L\Psi_3, \ldots, L\Psi_{Ne} \rangle \, d\Pi \quad (3-9b)$$

By using the system (3 – 9), the matrix will be obtained as names (K) called as stiffness matrix and then the matrix form can be transferred towards the system of equations with couple of unknowns. It is very complex problems because of the couple of unknowns involved into the same system. Therefore, choice is iterative technique for the good convergence and more accurate method as Newton's method.

Newton RAPHSON Method

The method is very simple and well-known technique since the invention in 2005 by Burden Fairs and too largely employed in vast fields of non – linear equations of various unknowns separately. This technique is just initiated through the best initial approximation of each known as (0, 0, 0, 0) and then the procedure is iterated up to the required accuracy level and terminate position. The initial technique general form is as below;

$$\lambda_{i+1} = \lambda_i - \frac{f(\lambda_i)}{f'(\lambda_i)} \qquad i = 0, 1, 2, 3, \ldots \qquad (3-10)$$

The formulation as (3 – 10) may be extended for more than one couple of equation system with various known components of fluid parameters that are described as;

$$\lambda_{i+1} = \lambda_i - J(\lambda_i)^{-1} f(\lambda_i) \qquad i = 0, 1, 2, 3, \ldots \qquad (3-11)$$

Though, $J(x_i)^{-1}$ can be obtained from the all differentials of the system of equations in two – dimensions (x and y) and is defined as inverse matrix and in real analysis, it is called as Jacobean matrix;

$$J(\lambda)^{-1} = \begin{bmatrix} \frac{\partial f_1}{\partial x_1}(\lambda) & \frac{\partial f_1}{\partial x_2}(\lambda)\ldots\ldots & \frac{\partial f_1}{\partial x_n}(\lambda) \\ \frac{\partial f_2}{\partial x_1}(\lambda) & \frac{\partial f_2}{\partial x_2}(\lambda)\ldots\ldots & \frac{\partial f_2}{\partial x_n}(\lambda) \\ . & . \quad \ldots\ldots & . \\ . & . \quad \ldots\ldots & . \\ . & . \quad \ldots\ldots. & . \\ \frac{\partial f_n}{\partial x_1}(\lambda) & \frac{\partial f_n}{\partial x_2}(\lambda)\ldots\ldots & \frac{\partial f_n}{\partial x_n}(\lambda) \end{bmatrix}$$

After computing the inverse matrix through various differentials of x and y, the formulation (3 – 11) may be initiated through the particular approximations and repeated until the required accuracy will be achieved and stopped up to the required termination level.

Computational Predictions of Non-Newtonian Fluids Through Two Step Rectangular Backward DUCT

The double step forward and backward channel study is newly studied numerically because of the severe need in the flow separations and especially reattachment length measurements in the dam flow phenomena like fixation a flumes and spillways channel to increase the heat transfer and extend the hydraulic jumps in the hydraulic engineering and irrigation canals. The application is not limited but extended in the solar plants reactors and diffusers and also required in the turbine blades in the field of the automotive and aircraft designing parts. Also, double step channel is highly needed in the shape of the ship air wake and flow moved through the pickup truck either liquid and solid material transported (Togun, et al. [2013] and Wang, et al. [2014]). Wang, et al. [2014] was designed the double step backward duct geometry by the aid of the CFD package ANSYS Fluent to examine the fluid dynamics of various parameters. The Reynolds average Navier–Stokes equations were studied for the turbulent flow phenomena with the selection of k –ε and k–ω turbulent models of finite volume iterative tool at the variety of the Reynolds number above 20, 000. Various cases of the reattachment lengths were computed as (d/h = 0 to 10) and formed five types of eddies at the different step corners of the backward step duct. The conclusions were focused that the different variations in reattachment lengths and eddies intensities of different locations formed and due to turbulent flows, the large number of eddies observed at the corners and splitted into the small eddies in size observed. Also, found the change in the quantitative values of the eddy intensities due to change the value of the Reynolds number. Togun, et al. [2013] was investigated air flow dynamics and heat generate via the double converging and diverging duct numerically with the adoption of the CFD packages ANSYS ICEM for the designing a complete mesh file and then exported to the ANSYS Fluent for the solver process and visualization process of flow features of double step duct. The impact of the increasing Nusselt number and limited Reynolds number extended for all cases were observed on the air flow patterns. Different influence on the flow and heat transfer was discussed as change in step height, variance in the Reynolds number with mean Nusselt number and different patterns of the streamlines. The results of the velocity streamlines justified that high heat transfer occurred because of the creation in the recirculation flow rate and showed the enhancement in the values of the Nusselt number because of the growing in the Reynolds number and increase step height. In this part, employed numerical methodology as finite element method with combination of least square tool for the solution of the velocity unknowns at different rates of the viscosity because of the change in behave of the fluids. The CFD tool COMSOL Multiphysics is chosen here for the CFD study of the fluid dynamics through the double step backward channel. For the physical unknowns, momentum brinkman equation in two–dimension is employed for the incompressible fluids and observed the laminar flow patterns due to change in the Reynolds number. Different types of the flow patterns are observed as streamlines for velocity at different power law indices rates, recirculation flow rate and eddy intensity with different tests of the Reynolds number.

Mathematical Model Definition and Concern Conditions

The geometry is chosen as three different sizes rectangles in different sizes combined as known as double backward step channel. Detailed number of zones as inlet, outlet and stationary walls are discussed in schematic diagram. Due to parabolic nature of the governing equations to fix parabolic inlet conditions at the inlet of the geometry as $u = f(y) = 10 \times \mathrm{U}_{\max} \times y(1-y)$. Also, other conditions at outlet and stationary walls are displayed at the diagram. Consequently, designed the finite element mesh of the domain and distribute into the various number of zones that detail is given as under;

Description	Value	Description	Value
Minimum element quality	0.7622	Maximum element size	0.008
Average element quality	0.9903	Minimum element size	1.6E-5
Triangular elements	7557	Curvature factor	0.2
Edge elements	321	Predefined size	Extremely fine
Vertex elements	8	Custom element size	Custom

Table – 1: statistics of the extremely fine mesh structure (FEM)

Findings of the Approximate Results

Here examined the FEM results of the velocity field at different values of the Reynolds number up to the limit of the laminar flow patterns (01 to 1500) and analyzed the behave of different kinds of fluids by computing the separate viscosity of each fluid through the power law model due to change index rate (n = 0.9 and 1.1). Diagram – A#1 is stated the complete sketch of the geometry in which defined the complete zones to enter the fluids and outflow the fluids with preferred the boundary conditions as no – slip boundary conditions at the all-solid walls. Diagram – A#2 are stated as mesh style of the geometry and developed three types of meshes consisting the weaker, finer and finally extremely fine for the final results of the velocity field. The discussion of the velocity field is stated as the impact of the Reynolds number on each power law indices rates and also stated the impact of the power law indices on selected Reynolds number.

Impact of the Reynolds number on velocity fields with constant index rate (n = 0.9)

The Reynolds number observed the fluid resistance and power law index rate stated behave of the fluids and focused on the non – Newtonian fluids. Diagram – A#3(a) stated the streamline laminar flow patterns of the shear thinning fluids at lowest Reynolds number (up to 200) in which observed two eddies as primary appeared in the first step and secondary eddy at second step. At lowest Reynolds number (=01), very smallest eddies (both) appeared at the silent corner of the backward step channel. When grows the value of the Reynolds number up to 200, the primary eddy is very slowly increased in size at first step and secondary eddy is also slowly increased in size but the size of secondary eddy is higher than the first eddy appeared in the corner of the backward step channel. Diagram –A#3(b) stated as same streamline flow patterns of the velocity field at greater values of the Reynolds number (200 to 500), the both eddies (primary and secondary) appeared in the corners of the steps in the backward channel and both eddies are increased in size other than the lowest Reynolds numbers. Successfully, Diagram – A#3(c) is stated the streamline patterns and observed the very long eddies in size at the Reynolds numbers 600 appeared in the corner of the backward step channel and grows the value of the Reynolds number (up to 950), the primary eddy is occupied the whole region of the first step and similarly the secondary eddy is fully occupied the whole region of the second step in the backward step channel because of the shear thinning behave of fluids and low viscosity fluids measured.

Impact of the Reynolds number on velocity fields with constant index rate (n = 1.1)

Here examined behave of thick type of fluids transported via double step backward channel at various tests of the Reynolds number with constant power law index rate (n = 1.1). Diagram – A#4 (a) is stated the streamline patterns of velocity moved the shear thickening fluids at lowest Reynolds numbers (01 to 200) and observed only small in size secondary eddy in the corner of the second step in the channel but diminished completely the primary eddy in the corner of the 1st step of the channel. Also, primary eddy is not appeared due to increasing Reynolds number (100) but the very slowly the secondary eddy size is increased and similarly the primary eddy is appeared after the Reynolds number (150) and finally observed at the Reynolds number (200), lowest in size the primary eddy initiated at the silent corner of the 1st step and secondary eddy is clearly visualized in the corner of the 2nd step of the channel. Diagram – A#4(b) stated the next streamline patterns at greater Reynolds numbers and observed the clear eddy structure in the corners of the double step channel. The primary eddy is too slowly increased and secondary eddy is moved towards the outflow in the double step channel. After that, diagram – A#4(c) is stated the clear visualizing picture of the eddies in the largest Reynolds numbers (1000 to 1500) and observed the full in size primary eddy appeared in the corner of the 1st step channel and completely filled the whole region of the 2nd step in the channel with the large eddy in size. Also, the eddy structure is very slowly observed in the corners of the double step channel due to very thick behave of the fluids.

Act of the Power law index rate on velocity fields with constant Reynolds number

Though, discussed here the streamline patterns of the two types of the fluid behave at the Constant Reynolds numbers (01 to 950). Diagram – A#5(a) is stated that primary eddy is not appeared in the corner of the 1st step at the constant Reynolds number (01 to 100) but the secondary eddy is appeared in the corner of the

2nd step but the size is almost same because of the lowest fluid resistant. Gradually, Diagram–A#5(b) illustrated the behave of the two fluids thinning and thickening fluids at the fixed Reynolds number and almost the behave of the fluids remained same as primary vortex did not appear and secondary vortex in size remained same appeared in the corner of the step in the backward channel at the values of the fluid inertia (01 to 100). Diagram – A#5(b) illustrated the more streamline patterns and eddies structure in sizes are almost same appeared in the corner of the double step backward channel at the value of the fluid inertia (=300) and clear impact is appeared in the sizes of the eddies in the corner of the double steps backward channel at the value of the Reynolds number (=500) that showed the primary vortex in size is higher in shear thinning fluids other than shear thickening fluids and similarly, secondary eddy in size also higher in thinning other than thickening fluids. Similarly, more tests of higher Reynolds number due to observe change in the eddy structure appeared in the corners of the double steps in the backward channel. Clearly appeared the impact of the power law index on flow features with fixed Reynolds number that illustrated that the primary eddy is very quickly filled the region of the 1st step in the thinning fluids other than thickening fluids, the primary eddy did not fill the region and similarly, the secondary eddy is highly moved towards the outflow in the channel at the value of the Reynolds number (=950) in the behave of the shear thinning fluids other than shear thickening fluids that very slowly moved towards the outflow of the channel in the Diagram – A#5(c). Another flow features of the maximum values of the Recirculation flow rate at all Reynolds number with imposed separately power law index rate (0.90 and 1.1) and illustrated that the recirculation flow rate is enhanced in both type of fluids with growing in the Reynolds number shown in the Diagram – A#6 (a and b) and visualised that the trend of increasing is observed higher in the shear thinning plot other than the shear thickening fluids plot. Similarly, Diagram – A#7 illustrated that the clear visualising picture of eddies structure that showed the eddy enhancement with grows in the Reynolds number and the enhancement in the thinning fluids observed higher than the thickening fluids. Consequently, the detail statistics of the minimum and maximum values of the recirculation flow rate and length of eddies with different Reynolds number and change in the power law index rate shown in the table – A#8 and A#9. It is highly needed to contribute in the research to develop here the empirical equations on recirculation flow rate with various Reynolds number by the least square analysis that are found as under;

Spectrum of Engineering Sciences
ISSN (e) 3007-3138 (p) 3007-312X Volume 3, Issue 9, 2025

Power law index rate (n=0.9) $01 \leq \text{Re} \leq 1500$

$$X = 7.193e - 07\,\text{Re} + 2.88e - 7$$

Power law index rate (n=1.1) $01 \leq \text{Re} \leq 800$

$$X = 2.8766e - 06\,\text{Re} + 3.8942e - 06$$

Summary

Successfully, Galekrin finite element solution is obtained for the all-physical unknowns through the momentum transport equation with couple of continuity equation in the Cartesian coordinates system. The governing equations are described in two – dimensions and focused on the non – Newtonian fluids transfer through the double step backward duct. Power law model is chosen for the computations of the viscosity of the fluids and change in the power law indices rates (n = 0.9 and 1.1). Also, various influences of the fluid inertia rates and change in the power law indices on fixed value of the fluid inertia. All approximate results are computed through the CFD plate form as COMSOL Multiphysics for the problem designing, developing the grid system and further visualize flow phenomena through the double step backward duct. Due to low Reynolds number (01), no any eddies observed at both power law indices (0.9 and 1.1) and slowly increased the size of the eddy because of the increasing Reynolds number on fixed power law indices (1.1) and quick enhanced the size of the eddy at the fixed power law index rate (0.9).

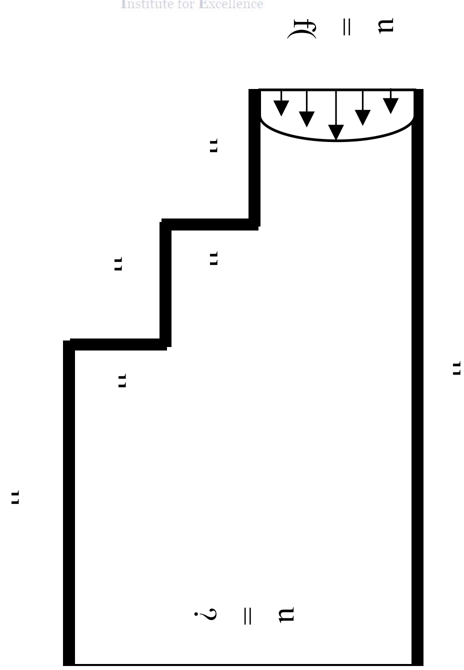

Diagram–A#1: Schematic diagram of the two-step rectangular backward step duct

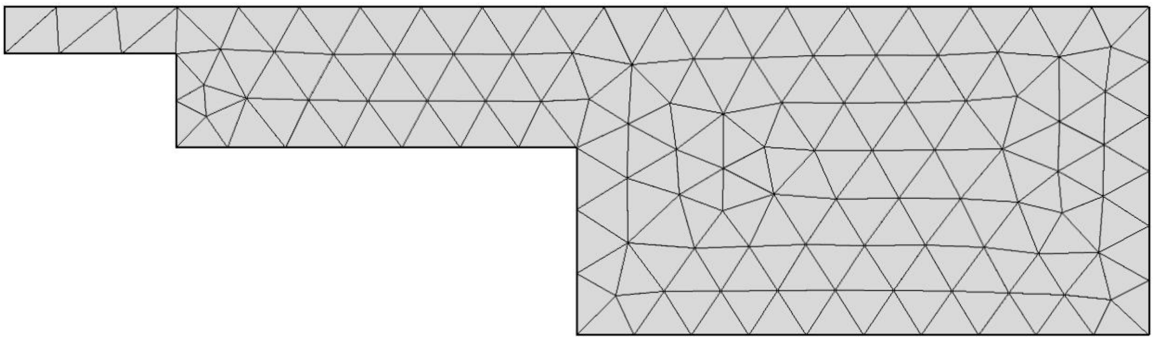

(a)

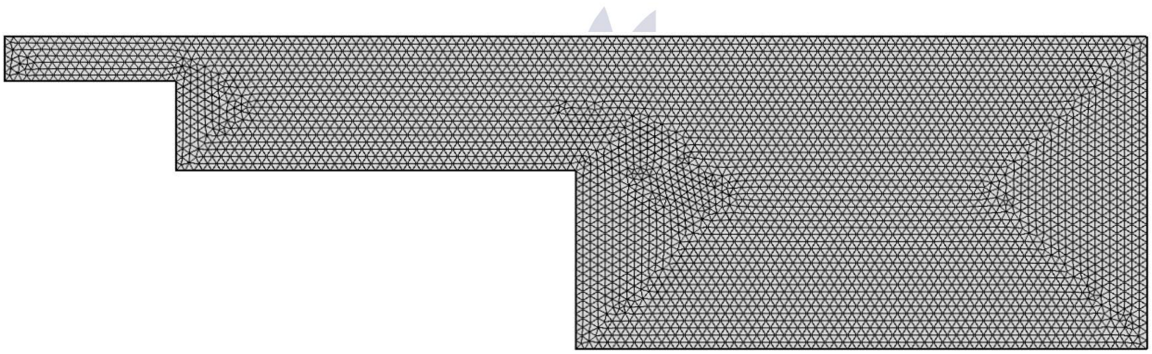

(b)

Diagram–A#2: Finer and extremely fine mesh of two step rectangular backward duct

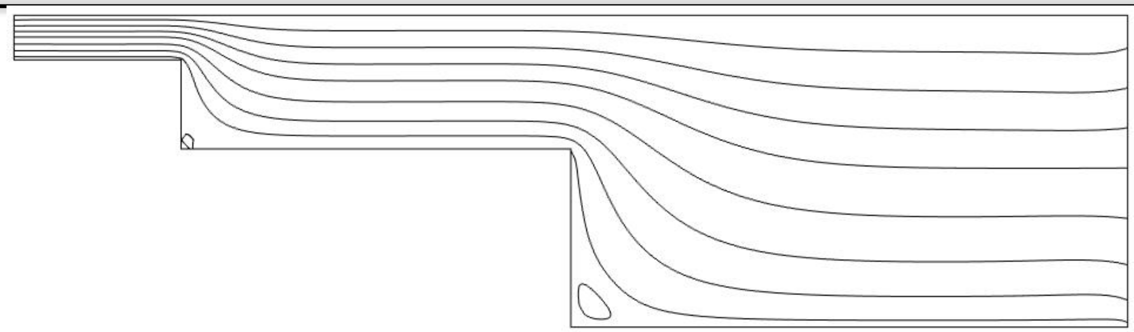

Re = 01

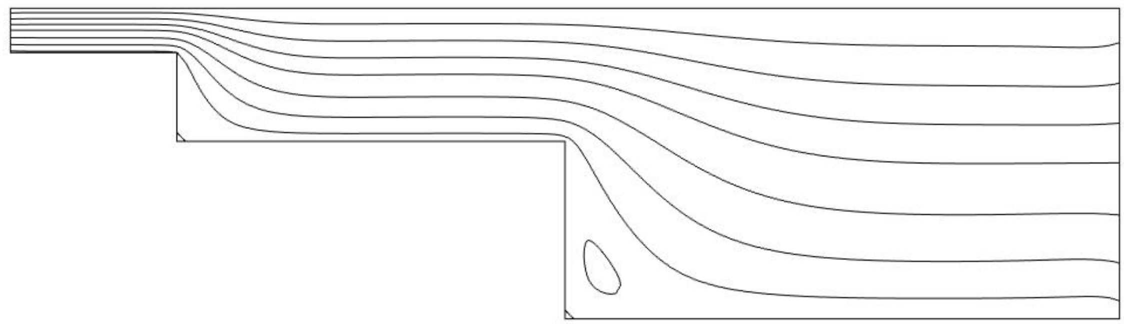

Re = 100

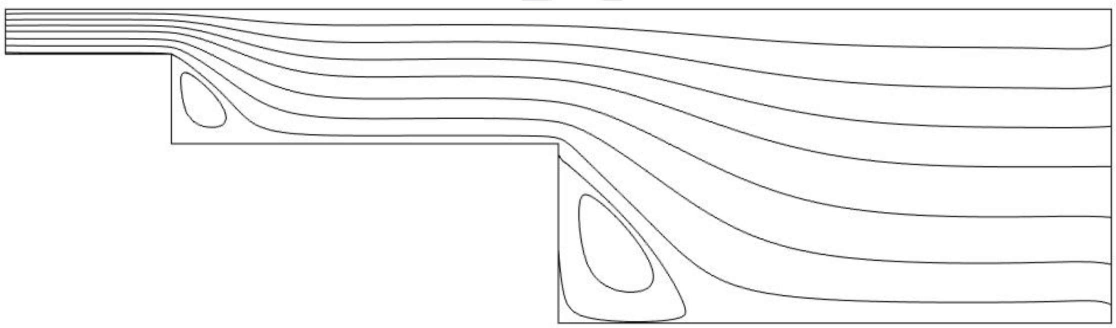

Re = 200

Diagram –A#3(a): Streamline Contours of Velocity of two step rectangular backward duct with fixed power law index rate (n) = 0.9

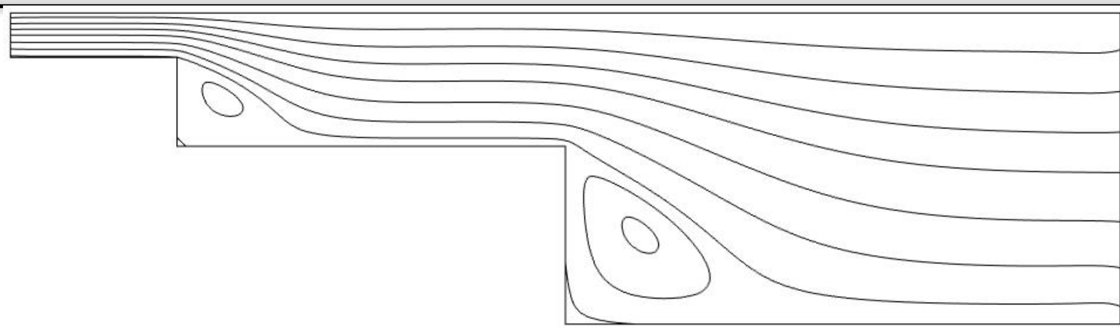

Re = 300

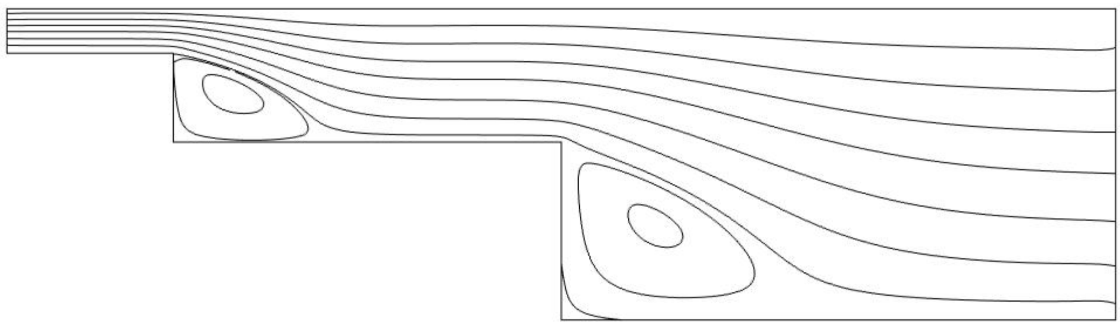

Re = 400

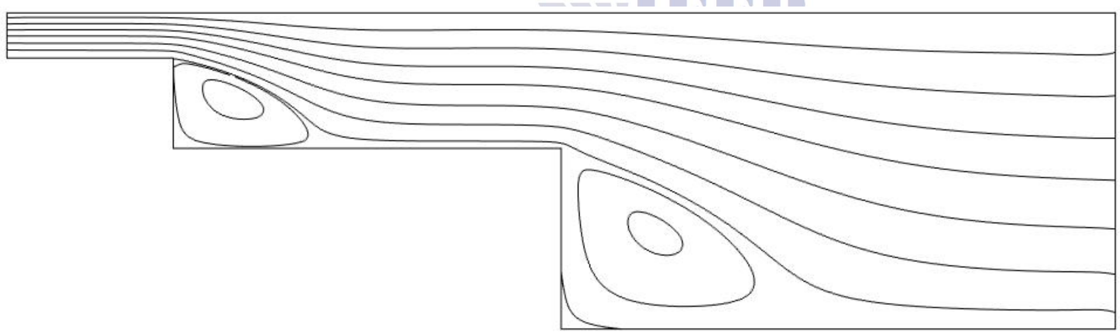

Re = 500

Diagram –A#3(b): Streamline Contours of Velocity of two step rectangular backward duct with fixed power law index rate (n) = 0.9

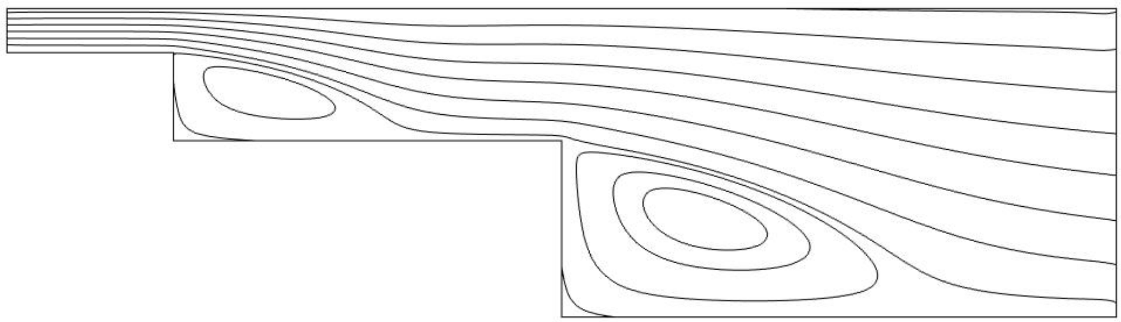

Re = 650

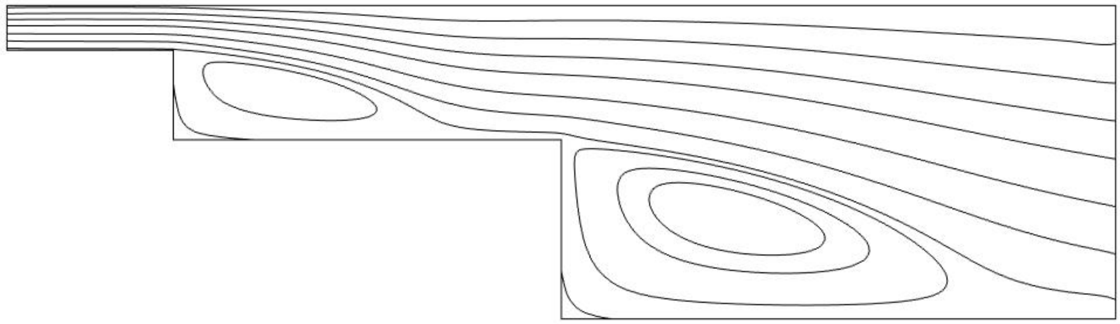

Re = 800

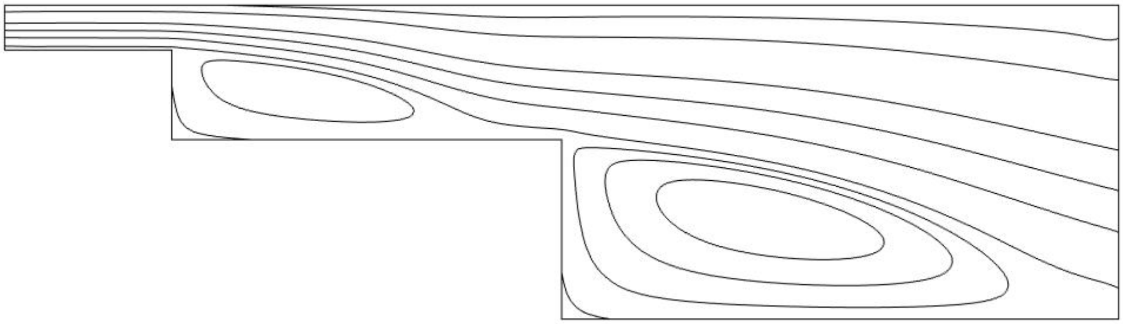

Re = 950

Diagram –A#3(c): Streamline Contours of Velocity of two step rectangular backward duct with fixed power law index rate (n) = 0.9

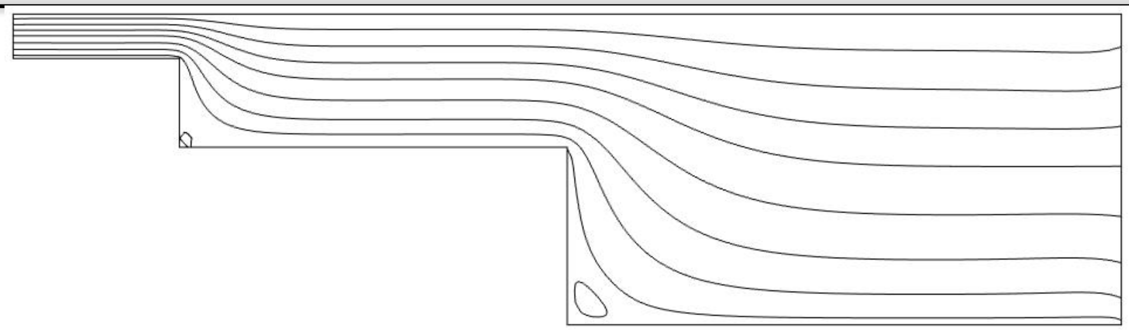

Re = 01

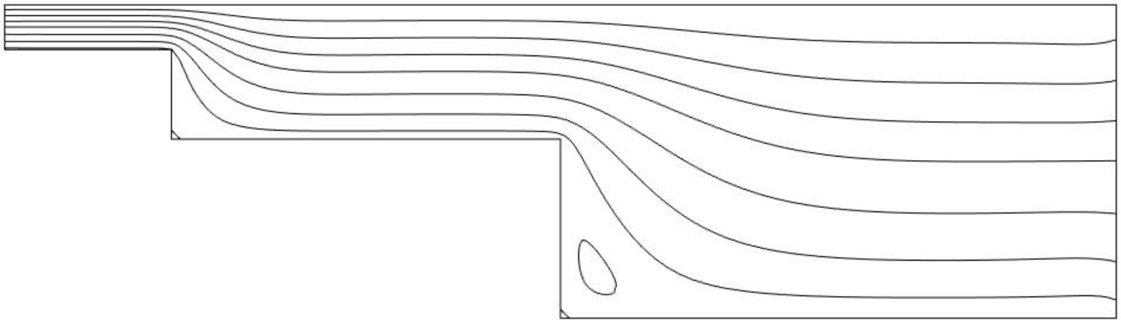

Re = 100

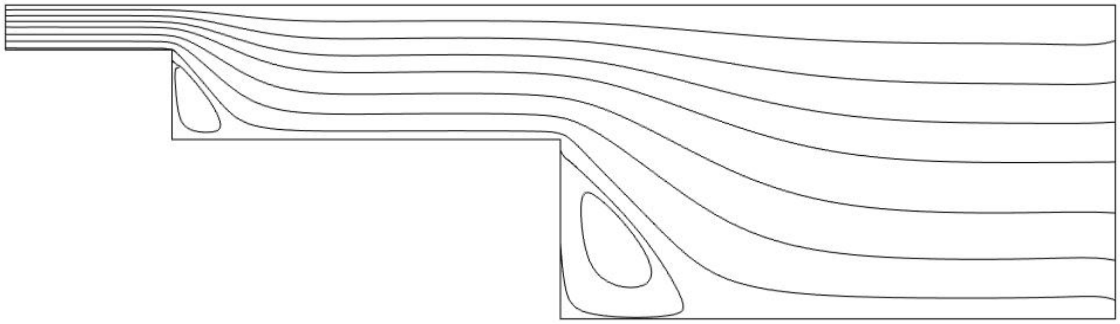

Re = 200

Diagram –A#4(a): Streamline Contours of Velocity of two step rectangular backward duct with fixed power law index rate (n) = 1.1

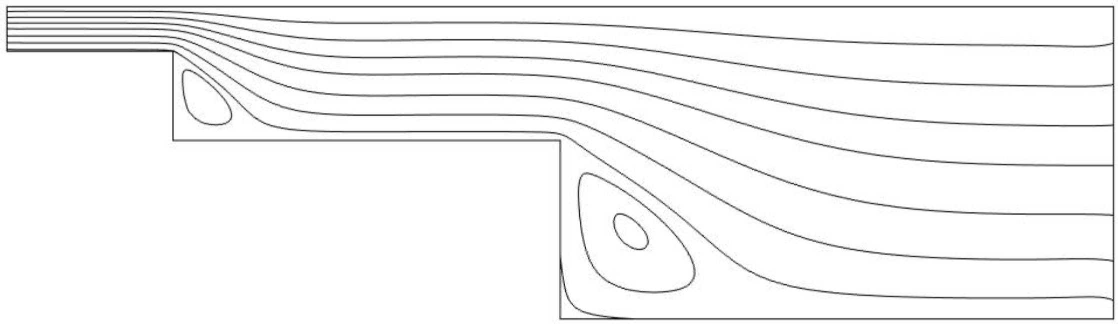

Re = 300

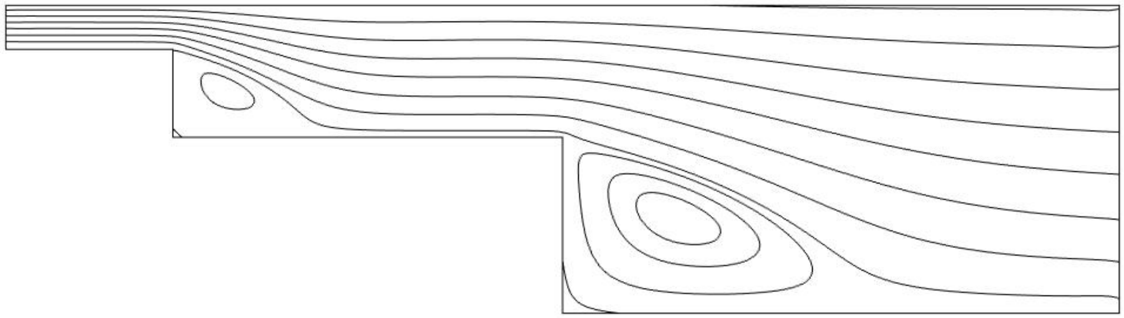

Re = 600

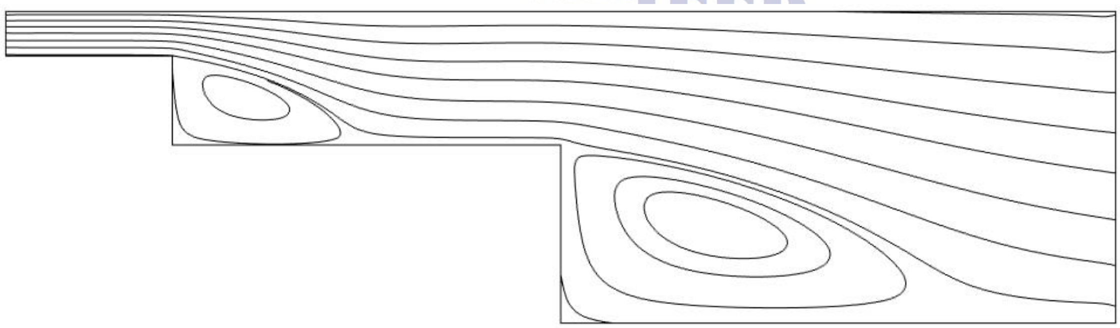

Re = 900

Diagram –A#4(b): Streamline Contours of Velocity of two step rectangular backward duct with fixed power law index rate (n) = 1.1

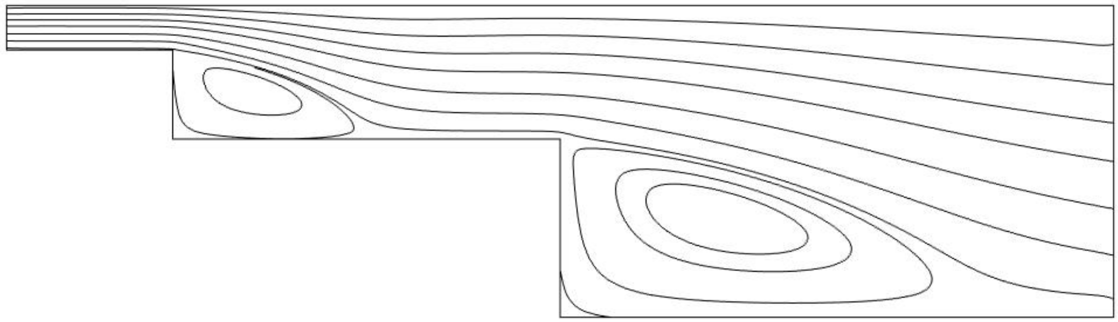

Re = 1000

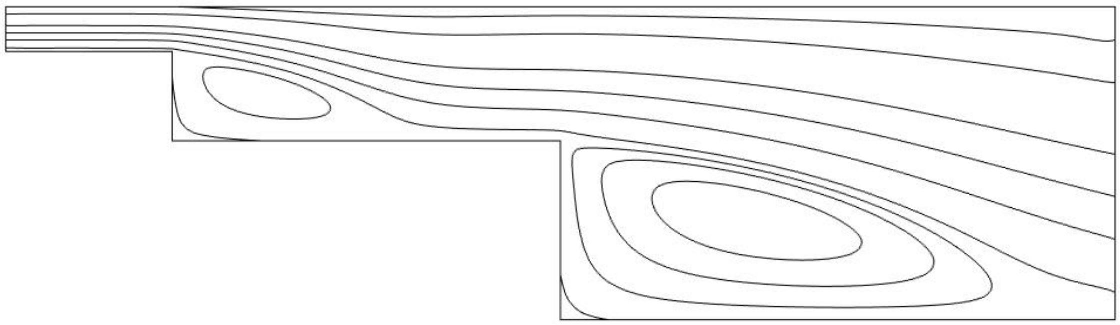

Re = 1250

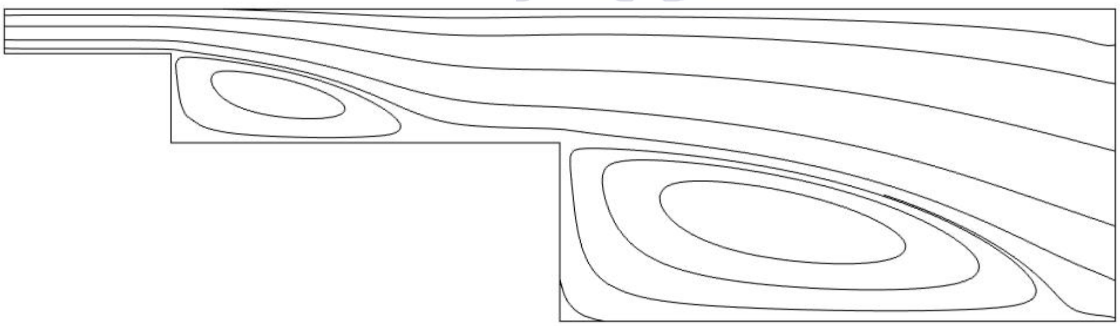

Re = 1500

Diagram –A#4(c): Streamline Contours of Velocity of two step rectangular backward duct with fixed power law index rate (n) = 1.1

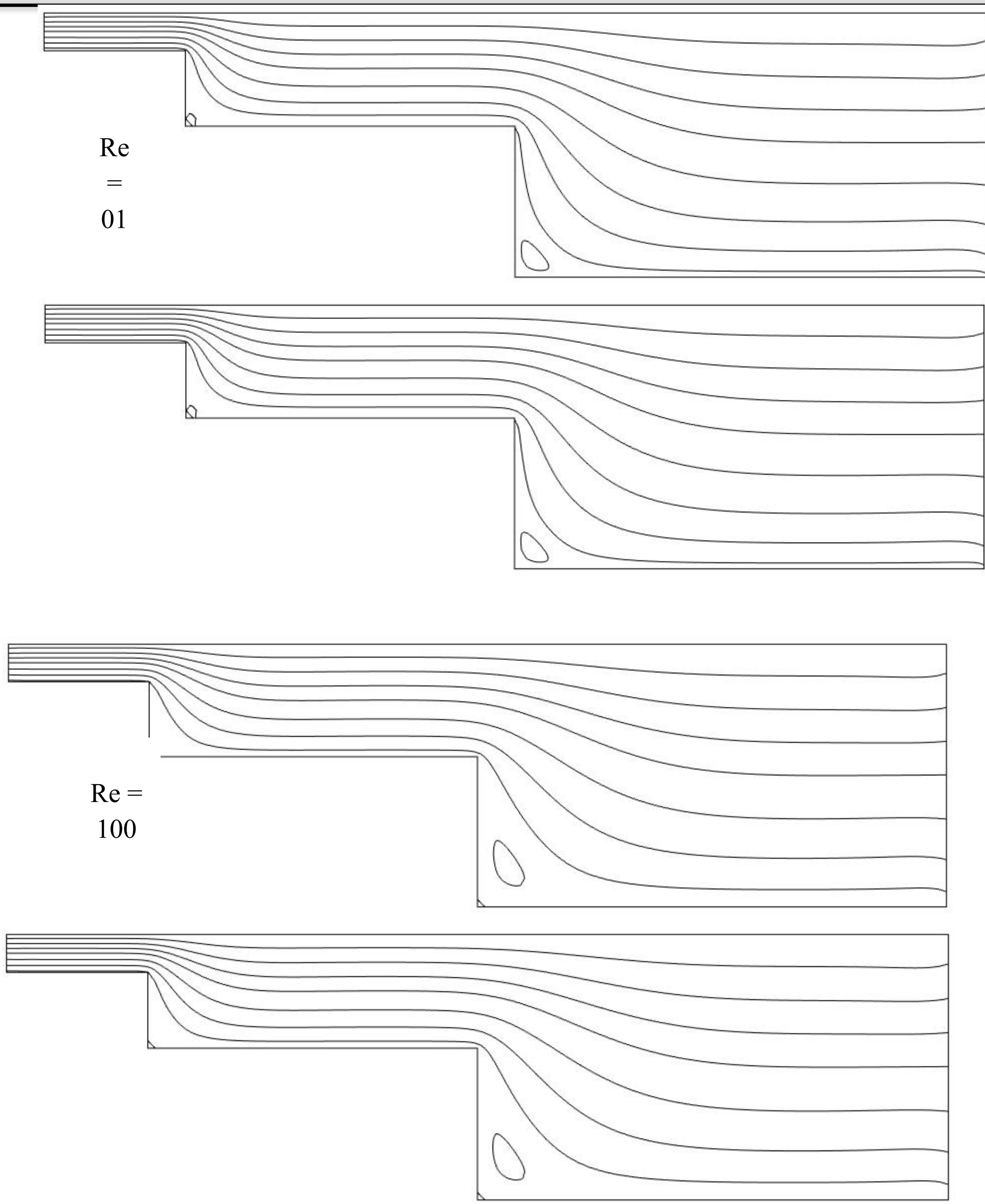

Diagram –A#5(a): Streamline Contours of Velocity of two step backward duct with fixed power law index rate at different values of the Reynolds number (01 to 100)

ISSN (e) 3007-3138 (p) 3007-312X Volume 3, Issue 9, 2025

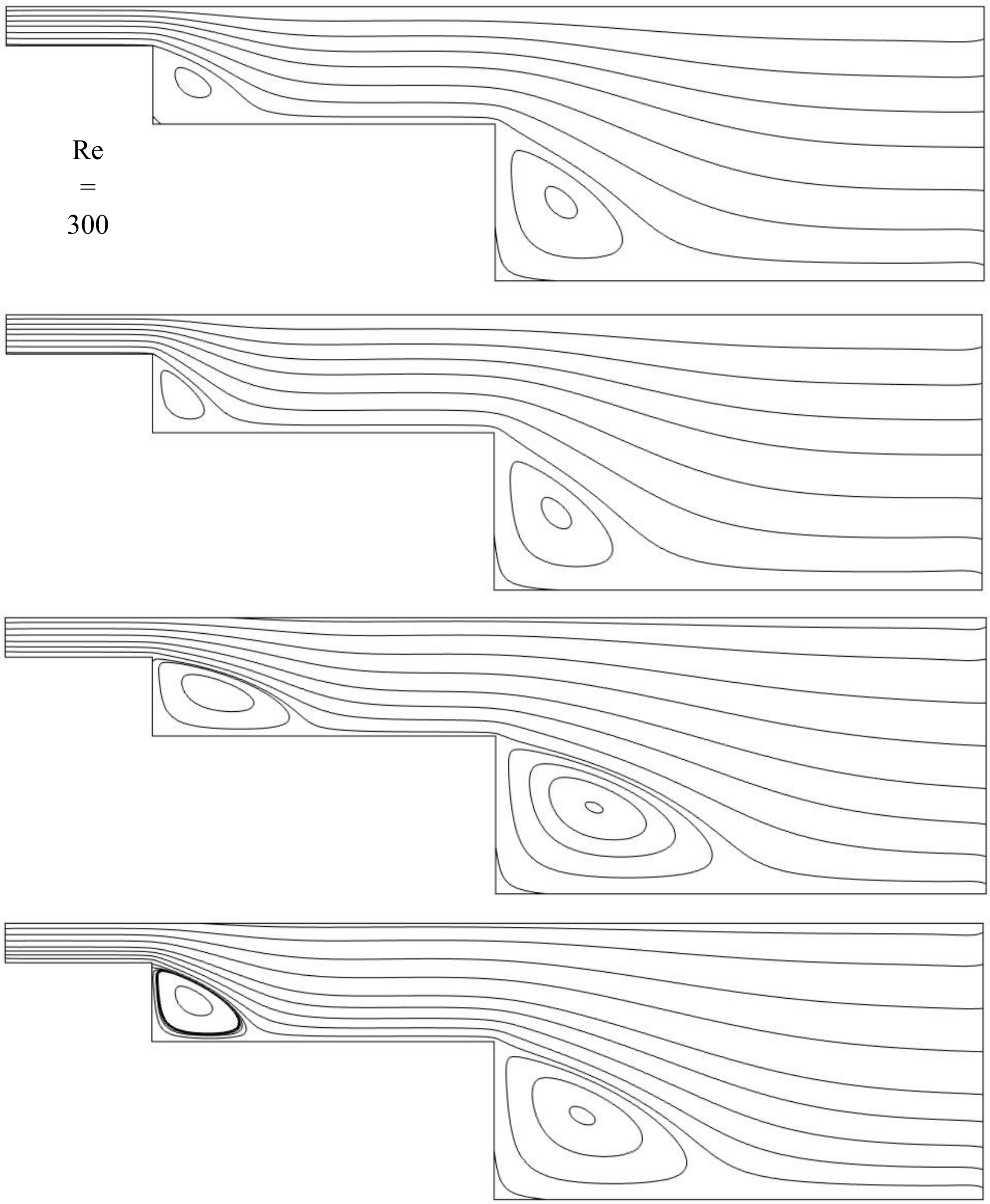

Diagram –A#5(b): Streamline Contours of Velocity of two step backward duct with fixed power law index rate at different values of the Reynolds number (300 and 500)

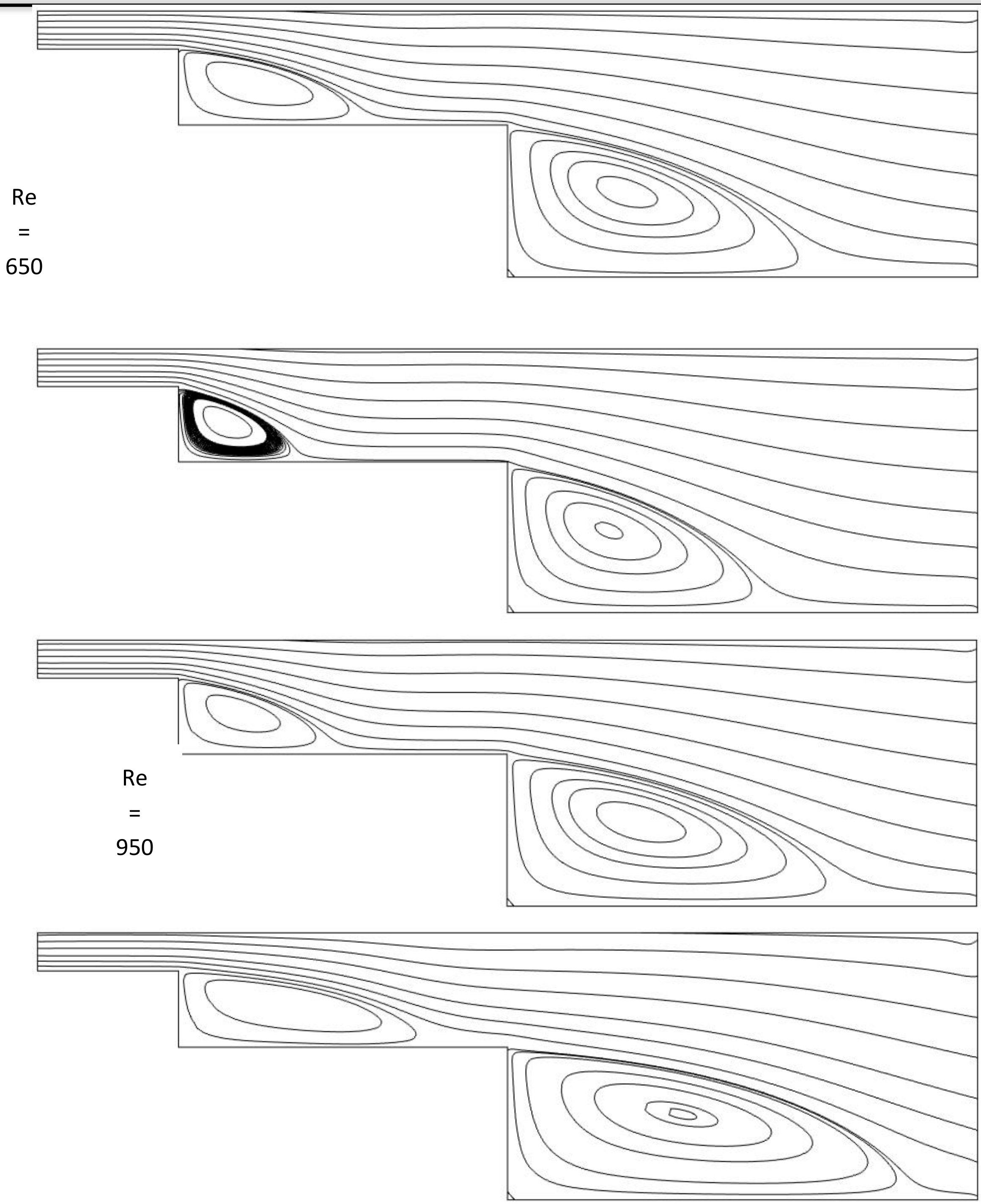

Diagram -A#5(c): Streamline Contours of Velocity of two step backward duct with fixed power law index rate at different values of the Reynolds number (650 and 950)

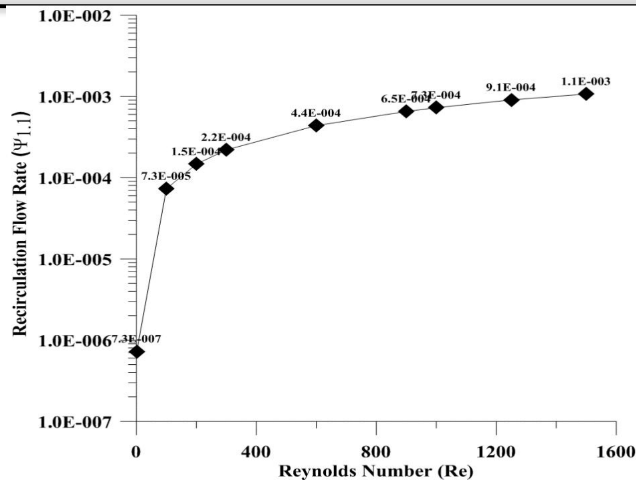

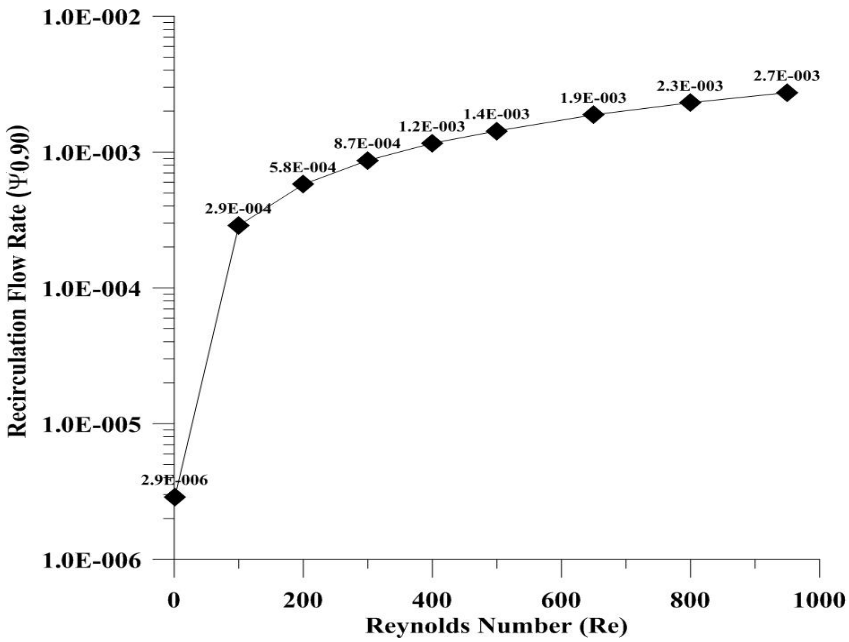

Diagram –A#6(a and b): Recirculation flow rate (Ψ) at various Reynolds numbers (Re) for the two-step rectangular backward duct

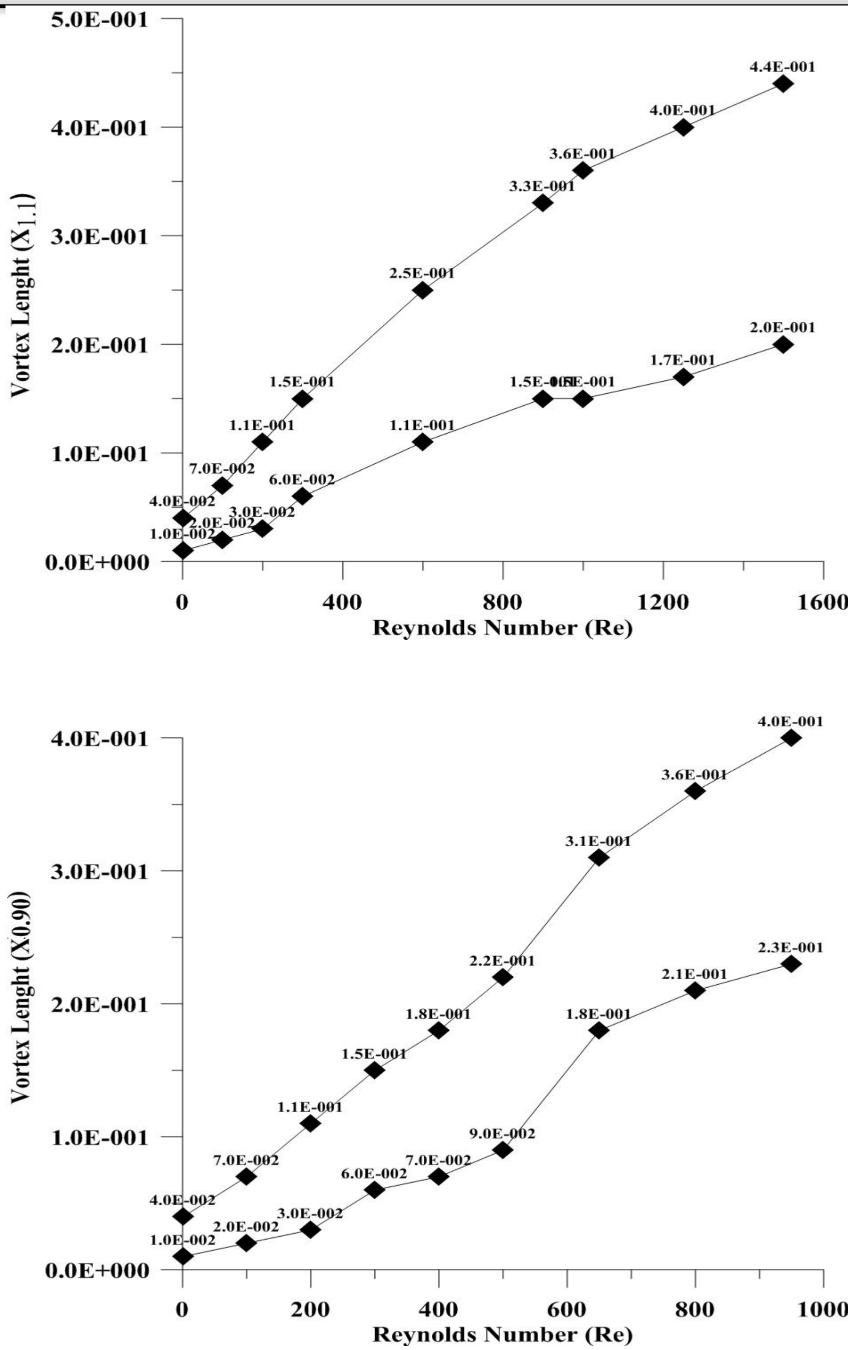

(b)

Diagram –A#7(a and b): Vortex length (X) at various Reynolds numbers (Re) for the two-step rectangular backward duct

Recirculation Flow Rate(Ψ)

Reynolds number(Re)	n = 0.90		Reynolds number(Re)	n = 1.1	
	(Ψ_{min})	(Ψ_{max})		(Ψ_{min})	(Ψ_{max})
01	4.49e-10	2.89e-6	01	1.2e-12	7.26e-7
100	8.96e-10	2.88e-4	100	1.91e-8	7.31e-5
200	2.11e-09	5.78e-4	200	1.32e-8	1.47e-4
300	1.66e-8	8.68e-4	300	4.81e-9	2.2e-4
400	2.16e-08	1.16e-3	900	8.6e-9	6.54e-4
500	2.3e-08	1.43e-3	1000	3.87e-11	7.27e-4
650	8e-11	1.88e-3	1250	6.09e-11	9.06e-4
800	2.55e-8	2.31e-3	1500	7.11e-9	1.07e-3

Table–A#8: Minimum and Maximum values of Recirculation flow rate at different Reynolds Number for two step rectangular backward duct.

Vortex Length(X)					
Reynolds Number (Re)	**n = 0.9**		**Reynolds number(Re)**	**n = 1.1**	
01	0.01	0.04	01	0.01	0.04

100	0.03	0.07	100	0.02	0.07
200	0.06	0.11	200	0.03	0.11
300	0.08	0.16	300	0.06	0.15
400	0.12	0.20	900	0.15	0.33
500	0.14	0.25	1000	0.15	0.36
650	0.18	0.31	1250	0.17	0.40
800	0.00	0.36	1500	0.20	0.44

Table–A#9: Vortex Length (X) at different Reynolds Numbers for two step rectangular backward duct.

Conclusion and Related Extension

Conclusion

Successfully, the numerical methodology is extended from Newtonian fluids towards non-Newtonian fluids. For the non-Newtonian fluids, the viscosity of fluids varies and computed through the most well-known model as POWER LAW MODEL. Only two type of fluids whose power law index rate is 0.9 and 1.1. Two fluids are tested with various range of the Reynolds number through two step backward step channels. The predicted results focused on the finite element method by the choice of the CFD package COMSOL Multiphysics. In which, Galekrin discretization is adopted for the conversion differentials appeared in the governing equations and control through the conversion higher order diffusion term towards first order system. For the first order system, applied mathematical algebraic procedure from the vector analysis to introduce the vorticity as an extra unknown with the couple of the velocity field. Through the COMSOL package, all meshes as weaker, finer and extremely fine meshes are tested for the approximate results but the successive results focused on the extremely fine mesh because of the accurate results and required level of convergence.

In the shear thinning fluids, the primary and secondary eddy is started at the lowest value of the fluid inertia and primary eddy is slowly increased but the secondary eddy is gradually increased at the step of the channel. Alternatively, in the shear thickening fluids, the flow features are changed as primary and secondary eddy is initiated at lowest value (higher than the shear thinning fluids) and secondary eddy is very slowly increased at the corner of the second step of the channel. The flow features are clearly justified the real physics of fluids. In the plots of the eddies lengths, clear justified the increase and decrease the size of eddies that matched with the streamline flow patterns

Related Extension Work

The domain may be extended to more than two steps as like spillways. The flow may be extended as laminar to turbulent and fluids may be tested more power law index rates. The upper stationary wall may be extended as symmetry to combine upper and lower backward step channel.

References

Amin, F. (2025). Binary Flaw Detection: A Security Analysis Paper. *International Conference on Artificial Intelligence and Cybersecurity.*

Amin, F., (2025). A Scalable Framework for Interpretable Binary Vulnerability Analysis Using Data Dependency Modeling. *In Proceedings of the International Conference on Artificial Intelligence and Cybersecurity (ICAIC 2025)*, 249 – 255.

Amin, F., But, M. A., Amin, I., & Khan, A. (2024). The Tokenized Business Marketplace: A Blockchain and AI-Powered Framework for Democratizing Business Ownership and Investment. *International Journal of Business and Management Sciences*, *5*(4), 318-328.

ı, F., Daudpota, N., & Khan, A. (2025). A Complete Penetration Testing Framework: Simulating Attacks and Evaluating Post-Exploitation Techniques with Kali Linux and Metasploit. *Spectrum of Engineering Sciences*, 386-407.

ı, F., Said, I., & Butt, M. A. (2025). AI-Based Cybersecurity Solutions: Securing Information and Privacy in the Evolving Digital Age. *Journal of Engineering and Computational Intelligence Review*, *3*(2), 142-158.

ıawan, S., (2016). "Backward-Facing Step Geometry for Flow Analysis: A Review of Non-Dimensional parameters", Mechanical Engineering Dept. Universitas Tarumanagara, Volume#01.

, A., Amin, F., Sahoo, S. K., & Mishra, S. K. (2025). Secure comparative evaluation of Alzheimer MRI classification models using blockchain. In *2025 13th International Conference on Intelligent Systems and Embedded Design (ISED)* (pp. 905-911). IEEE.

P, Weiss , Deck, S., Robinet, J.C and P. Sagaut, (2014). "On the dynamics of high Reynolds number turbulent axisymmetric and plane separating/reattaching flows", Onera, Applied Aerodynamics Department, Missiles Hypersonic Launchers Unit, 8, rue des Vertugadins, Meudon, France.

S.D and Barber, T.J. "A Detailed CFD and Experimental Investigation of a Benchmark Turbulent Backward Facing Step Flow", University of NSW, Sydney, Australia.

ıe, A., Ahmad, F., Yamada, S and Chaudhry, S.R. (2007). "Assessment of Turbulence Models for Turbulent Flow over Backward Facing Step, Proceedings of the World Congress on Engineering 2007", Vol-II.

ız, U., Ahmad, B., Sajid, M. H., Abbas, Q., Qureshi, M. A., Rasheed, S., & Khan, A. (2025). An Integrated Machine Learning Framework for Structural Health Monitoring of Bridges: A Case Study on Soan Bridge. *The Asian Bulletin of Big Data Management*, *5*(2), 194-207.

Imtiaz, U., Malik, S., & Khan, A. (2024). Blockchain-Driven Cybersecurity Framework for Smart Homes: Integrating IoT and Machine Learning for Secure Automation. *The Asian Bulletin of Big Data Management*, *4*(4), 570-583.

Kwon YW, Bang H (2000) The finite element method using MATLAB, 2nd edn. CRC Press, Boca Raton

Shah, S. M. H., Amin, F., & Khan, A. (2025). Cyber-Resilient Mobile Edge Computing: A Deep Neural Approach for Secure and Efficient Task Offloading. *The Asian Bulletin of Big Data Management*, *5*(1), 200-215.

Smirnov, E.M, Smirnovsky, A. Schur1, N.A, Zaitsev, D.K and Smirnov, P.E. (02016). "Numerical simulation of turbulent heat transfer past a backward-facing step: 2D/3D rans versus iddes solutions", St.-Petersburg Polytechnic University, St.-Petersburg, Russia, ansys Germany , Otterfing, Germany, Journal of Physics: Conference Series.

Soma, R., Sahoo, S. K., Amin, F., & Mishra, S. K. (2025). A Federated Learning Framework for Multi-Parameter Optimization in Edge Computing. In *2025 13th International Conference on Intelligent Systems and Embedded Design (ISED)* (pp. 1-6). IEEE.

ey, C.E and Ukeiley, L.S., (2009). "A study of a 3-D double backward-facing step", Department of Aerospace Engineering and Engineering Mechanics, The university of Texas at Austin and Department of Mechanical and Aerospace Engineering, Research and Engineering Education Facility, the university of Florida.

ın, H, Ab.Razzaq, T, Kazi, S.N, Badarudin, A and Ariffin, K.A (2013). "Heat Transfer to Laminar Flow over a Double Backward-Facing Step", International Journal of Mechanical and Mechatronics Engineering Vol:7.

o, D. and Bung, D.B., (2015). "Hybrid Investigation Of Air Transport Processes In Moderately Sloped Stepped Spillway Flows", Research Assistant, FH Aachen University of Applied Sciences, Aachen, Germany, Professor, FH Aachen University of Applied Sciences, Aachen, Germany.

g, S., D. Burton, D. and Sheridan, J., (2014), "Characteristics of Flow over a Double Backward-Facing Step", fluids laboratory for Aeronautical and Industrial Research (FLAIR) Department of Mechanical and Aerospace Engineering. 19th Australasian Fluid Mechanics Conference. Melbourne, Australia.

ırich, D. Chanson, H. and Hydraulics, J. Hydraul. (2014). "Air Entrainment, and Energy Dissipation on a Gabion Stepped Weir"